Fundamentals of Wind-Tunnel Design

Louis Cattafesta, Chris Bahr, and Jose Mathew
Department of Mechanical and Aerospace Engineering, University of Florida, Gainesville, FL, USA

1 INTRODUCTION

Wind-tunnel testing of full/model-scale components is a widely employed technique that guides detailed design decisions in thermal-fluid systems and allows for fundamental research of fluid phenomena. Many instances occur where theoretical and/or computational techniques are inadequate, either due to the complexity of the problem or the lack of suitable computational resources. Wind-tunnel testing often serves as the most cost-effective approach for these reasons, as well as the expenses involved in many forms of full-scale testing (which can be related to wind-tunnel tests through appropriate parameter matching).

Wind tunnels are extensively used in research institutes, universities, industry, and governmental agencies for a wide variety of applications and can be classified in many ways. From a fundamental viewpoint, one can look at the dimensionless form of the governing equations of fluid motion, which contain various dimensionless parameters: Strouhal number *St*, Reynolds number *Re*, Euler number *Eu*, and Froude number *Fr*. When the energy equation is considered, additional dimensionless parameters appear, such as the Eckert number *Ec*, Mach number *M*, and Prandtl number *Pr*. Additional dimensionless parameters also appear due to boundary conditions, etc.

Wind tunnels can also be classified based on their operational flow regime and corresponding relevant dimensionless parameters. It is common to characterize an incompressible gaseous flow, such as air, primarily by its Reynolds number. Compressible gaseous flow is primarily characterized by its Mach and Reynolds numbers. Liquid flows are characterized primarily by the Reynolds and Froude numbers. These parameters are critical, as one of the key, though often unrealizable, goals of wind-tunnel testing is dynamic similarity, where all relevant dimensionless parameters match between model and full scale.

From a practical viewpoint, wind tunnels are often classified according to size. For example, low-speed ($M < 0.3$) wind tunnels vary from small tunnels (i.e., test sections with dimensions less than approximately $1\,\text{m} \times 1\,\text{m}$) to large tunnels capable of testing full-scale automobiles and trucks and large models of aircraft components. High-speed transonic and supersonic wind tunnels are also fairly common, but due to power requirements, these tunnels are typically relatively small in size compared to their low-speed counterparts.

Wind tunnels are also classified according to application. Some examples include tunnels with moving ground planes for automotive testing, icing tunnels for studying the effects of ice formation on aircraft wings, climate tunnels for simulating various environmental conditions, smoke tunnels for

Encyclopedia of Aerospace Engineering.
Edited by Richard Blockley and Wei Shyy
 ISBN: 978-0-470-68665-2

flow visualization, propulsion tunnels for the evaluation of aircraft engines, spin tunnels to study the spin recovery of an aircraft, and stability tunnels to study flight dynamics (Barlow, Rae and Pope, 1999).

As mentioned above, the key dimensionless parameter of interest in low-speed wind-tunnel tests is usually the Reynolds number, which is the ratio of inertial to viscous forces. For models exhibiting dynamic similarity, the forces and moments on full-scale models can be obtained by scaling the force and moment data. However, achieving Reynolds number similarity is a difficult task, even in incompressible flows. Since tunnel power scales with $\rho V^3 A_{\mathrm{TS}}$, restrictions on power consumption and available space often limit A_{TS}. Blockage constraints, in turn, limit model size. Assuming an air medium near standard conditions, the only way to match *Re* is to increase the tunnel velocity. In some cases, either a limit on maximum tunnel speed or the introduction of compressibility effects precludes *Re* matching. Thus, one is forced to accept the largest *Re* that can be achieved in the test section. Depending on the experiment of interest, this limit may or may not harm the validity of the results. This scenario is commonplace in small-scale aeroacoustic wind tunnels (Mueller *et al*., 1992; Mathew, 2005).

A quality aerodynamic wind-tunnel facility should provide a reasonable *Re* range, flow uniformity, and low turbulence intensities. In addition, aeroacoustic (Duell *et al*., 2002) and laminar-to-turbulent transition tunnels (Choi and Simpson, 1987) should also provide low background noise and vibration levels.

2 FACILITY CHARACTERISTICS

The following sections discuss several primary wind-tunnel characteristics that define a facility. Essential references for these characteristics and the ensuing design process can be found in the following: Barlow, Rae and Pope (1999), Pope and Goin (1965), and Mehta and Bradshaw (1979).

2.1 Drive system

A defining characteristic is the tunnel drive system, which determines how the working fluid is moved through the test section. Different drive systems have distinct optimum operational modes, whose selection is dependent on the medium and the operational regime.

For an air tunnel, two primary drive systems are a compressor and fan. In the former, pressurized air is supplied from a compressor (usually from storage tanks) through a controlled valve or regulator to the tunnel. In the latter, axial or centrifugal fans or blowers either push or pull air through the test section. Fans/blowers can be either shaft- or belt-driven, depending on acceptable costs and desired performance characteristics.

Compressor-driven facilities can provide large pressure ratios for relatively little cost and are often preferred for high-speed facilities that require high stagnation pressures. The trade-off is the fixed amount of air available for a test. Since typical compressors cannot supply the continuous mass flow necessary, these tunnels often limit the duration of an experiment to a few minutes or less, depending on the initial pressure, storage tank volume, and mass flow rate. Fan-based systems can operate continuously, but the cost scales dramatically with volume flow rate and power requirements. Fans tend to work best with low-speed facilities. An example compressor-driven facility is NASA Langley Research Center's 20-inch Supersonic Wind Tunnel (NASA Langley Research Center, 2006). NASA Langley's $14' \times 22'$ Subsonic Tunnel is a larger, fan-driven facility (NASA Aeronautics Test Program, 2007b).

2.2 Operating fluid

When dynamic similitude is difficult to achieve, several options are available. First, the working fluid of the tunnel can be changed from that of the full-scale application. However, when the working fluid is not the ambient fluid or matched to ambient conditions, for example, pressurized air, or water, a closed-circuit facility must be used and properly sealed to avoid leakage.

Another option is to use a pressurized gas as the working fluid. For a given temperature, this leads to a density increase that facilitates Reynolds number matching. Allowances must be made for the increased dynamic loading, proportional to dynamic pressure $0.5\rho_\infty V_\infty^2$, when density is dramatically increased. NASA Ames' $11' \times 11'$ Transonic Wind Tunnel is an example of a pressurized air tunnel (NASA Aeronautics Test Program, 2007a).

Alternatively, flow properties can be altered by cooling the *gas* medium. This can be done using a cryogenic system to increase fluid density and reduce the viscosity. Such facilities require significant thermal insulation, as well as large-scale refrigeration systems. NASA Langley's National Transonic Facility is an example of such a wind tunnel (NASA Aeronautics Test Program, 2007c).

For experiments involving two-phase flow, cavitation phenomena, or general maritime interest, a water tunnel can be used. Water tunnels must again be sealed against leakage and generally use pumps for operation. Maintenance costs may be significantly higher, depending on the ability to iso-

late contaminants from the flow reservoir. As with the previous alternative-fluid-facility-types mentioned, water will dramatically increase model loading for a given flow speed. The Garfield Thomas Water Tunnel Facility at Penn State University is an example of a large-scale water tunnel (The Pennsylvania State University, 2007). Free-surface wind tunnels are used to study air–water interfaces, and consist of both an air tunnel and a water tunnel, with a joined test section between the two (Rasmi, 2002). Tow-tanks are used for a variety of maritime applications and consist of large water tanks through which models can, as the name implies, be towed (Naval Warfare Center Carderock Division, 2009).

2.3 Duct circuit

Wind tunnels can be designed with two primary types of duct circuits: open or closed (Figure 1). An open-circuit facility ingests air from ambient at one end of the tunnel circuit, passes it through the tunnel, and exhausts to ambient. Closed-circuit tunnels retain a fixed mass of air, not accounting for leakage, and circulate flow in a loop through the various wind-tunnel components.

Open-circuit tunnels have generally lower fabrication costs and occupy less space. Since they constantly cycle in fresh fluid, localized seeding for flow visualization in the test section is straightforward. Purging injected seed particles is simple. One disadvantage is that, for a given speed, an open-circuit tunnel usually requires more energy for operation (Barlow, Rae and Pope, 1999). Also, significantly more flow conditioning may be required to reach flow quality comparable to an equivalent closed-circuit tunnel. The tunnel inlet and exhaust regions must be free of any obstructions. More seeding material is required for flow visualization as there is no simple mechanism to recycle the seeding particles. Depending on tunnel design and location, operation is dependent on local weather conditions. An alternative to controlling the flow conditions (temperature and relative humidity) is to house the wind tunnel in a large closed room with an HVAC system that has a larger capacity than the load imposed by the wind tunnel.

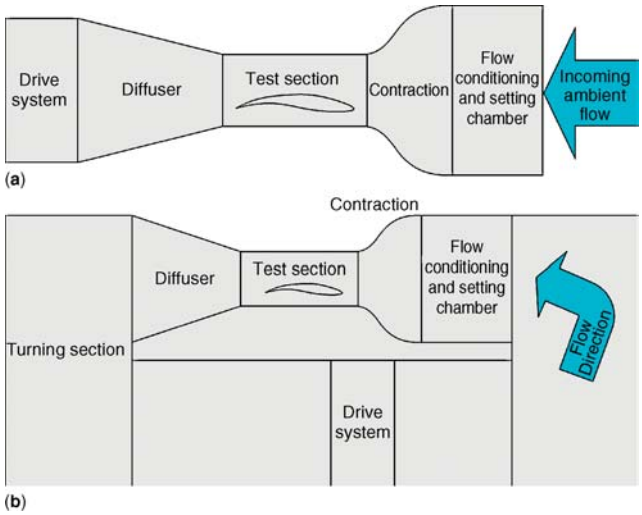

Figure 1. Schematic of (a) open-; (b) closed-circuit wind tunnels.

Closed-circuit facilities, while having additional construction expense, have lower operating costs than open-circuit facilities under similar operating conditions. While purging seed material requires more effort, less material is required for a given experiment. On the other hand, the seed quickly creates a homogeneous "fog" in the tunnel, allowing for uniform but global (as opposed to localized) seeding. The tunnel in most cases operates independently of local weather, and flow conditioning is simpler as the input flow conditions are regulated to a greater extent. However, due to the recycling of air through the drive system, which is often located "in line" with the flow passage to provide cooling, thermodynamic properties can change with air heating unless a flow cooling control system is employed.

2.4 Operational flow regime

A final major distinguishing characteristic of wind-tunnel facilities is the regime of operation. This is determined by the desired experimental niche of the facility and plays a strong role in the design.

Supersonic facilities ($M > 1$) have high energy and development costs. The facility must be designed to sustain large internal loads from high-pressure differences across the walls and (for hypersonic flow) potentially high temperature, as well as forces generated by both stationary and moving shock waves. The test section must be designed with an appropriate converging–diverging nozzle for the supersonic Mach number of interest to minimize shock wave generation and sized such that reflected shocks from a test model do not interfere with any experiments (see Complex Internal Compressible Flows). Instrumentation must be selected to withstand a large variety of conditions. Often tunnel size is reduced for larger Mach numbers to reduce energy costs.

Transonic facilities ($M \sim 1$) simulate cruise conditions for many civil and military aircraft. The flow around the model under test may reach local supersonic conditions, but the overall flow field in the test section may still exhibit subsonic, elliptic behavior. Slotted walls are usually used to accommodate shock waves with steep angles. Model scales are often significantly increased compared to supersonic facilities due

to the desire to achieve Reynolds number similarity. Thus, energy costs are still significant. Ejector systems are used to get the test section into the transonic range, as conventional inlet schemes for both subsonic and supersonic wind tunnels do not perform well (Bradshaw and Mehta, 2003).

Subsonic facilities are used to simulate flight by slower aircraft or examine take-off or landing configurations for larger aircraft. Ground vehicle facilities also fall in this category. Some facilities operate at or close to full scale, while smaller tunnels are necessarily restricted to small-scale testing. As mentioned above, for sufficiently low operational speeds ($M = 1$), the flow is essentially incompressible and M similarity is not required.

3 WIND-TUNNEL DESIGN

Wind-tunnel design is a process where research goals are first set, which then establishes the design criteria. Because the design typically involves fabrication, cost, space, and other conflicting constraints, the process is iterative.

3.1 Design criteria

Wind-tunnel design should be tailored to meet the specific research goals and is subject to budget and facility space limitations. Guidelines for the detailed design of wind-tunnel components are provided in this section, including flow conditioners, contraction, test section, diffuser, tunnel driver, and optional components. Interested readers should refer to dedicated texts on this topic (Barlow, Rae and Pope, 1999; Bradshaw and Mehta, 2003).

3.1.1 Research goals

A good wind tunnel should enable measurements of accurate steady or unsteady data, depending on the desired application. The turbulence intensity in the test section should be low enough to facilitate study of the physical phenomena of interest. For example, boundary-layer transition experiments (Saric, Reed and White, 2003) often require extremely low turbulence levels. Aeroacoustic experiments of trailing edge noise require low turbulence levels to minimize the effects caused by the impingement of freestream turbulence on the leading edge of a model (Mueller *et al*., 1992). The test section flow should be uniform and devoid of any unintended unsteadiness, while secondary flow effects should be minimized in the contraction. Flow separation should be avoided inside the tunnel circuit to prevent flow unsteadiness and associated noise, as well as to minimize losses. Blockage effects due to the test section model and the corresponding streamline curvature should be minimal to emulate freestream conditions. Vibrations generated by the drive system should be damped to minimize its influence on the experiment. In the case of aeroacoustic facilities, acoustic treatment is essential to minimize disturbance noise from contaminating the acoustic measurements.

3.1.2 Design process

The design of a wind tunnel is usually constrained by budget, operational and maintenance costs (see Project Management: Cost Analysis), and the overall size of the facility. A flow chart for the design of a low-speed, low-noise facility is shown in Figure 2. In low-speed facilities, Reynolds number considerations typically drive the test section size to its maximum value, subject to cost and size constraints. Test section size and desired flow quality determine the size of the flow-conditioning section. Trade-offs are often required between the desired inlet contraction ratio and contraction length in order to approach the required test section flow conditions while remaining within allowable dimensions. The inlet size determines the size of the settling duct that houses flow conditioners such as the honeycomb and screens. The honeycomb affects the flow uniformity, and the screens and subsequent settling duct length dictate the turbulence intensity in the test section. The diffuser should be designed to maximize pressure recovery from the losses incurred by the test section, contraction, and flow conditioners. Although a longer diffuser provides greater pressure recovery, size limitations often constrain the diffuser length and height. Some tunnels may require multiple diffusers connected by turning sections to fit within facility constraints, as assumed in Figure 2. Care must be taken to ensure no flow separation occurs in the ducts, which may also require acoustic treatment to minimize flow noise. The drive system must provide the desired flow rate and pressure drop requirements while maintaining reasonable energy efficiency. In a closed-circuit tunnel, the flow ultimately is routed back to the flow conditioners in front of the contraction, while in an open-circuit the flow exhausts to the ambient.

3.2 Component design guidelines

This section describes the design of various tunnel components, including the flow conditioners, contraction, test section, diffuser, and wind-tunnel drive. Optional components such as a turning section, vibration isolator, and jet collector for open-jet test sections are also discussed.

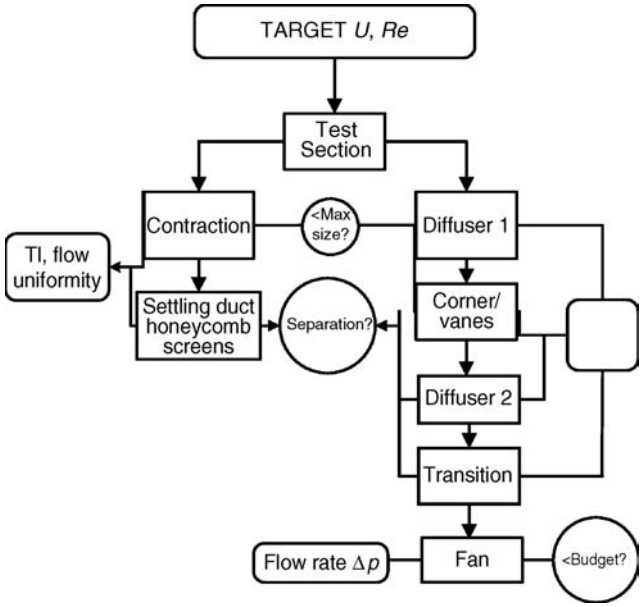

Figure 2. Flow chart for low-speed, low-noise, wind-tunnel design.

3.2.1 Flow conditioners

In most tunnels, the flow-conditioning section contains a honeycomb, screens, and a settling duct. An example honeycomb section is shown in Figure 3. The honeycomb aligns the flow with the axis of the tunnel and breaks up larger-scale flow unsteadiness. The screens cascade large-scale turbulent fluctuations into smaller scales. These decay in the settling duct, which must be sufficiently long to allow for sufficient decay while minimizing boundary-layer growth (see Turbulent Boundary Layers).

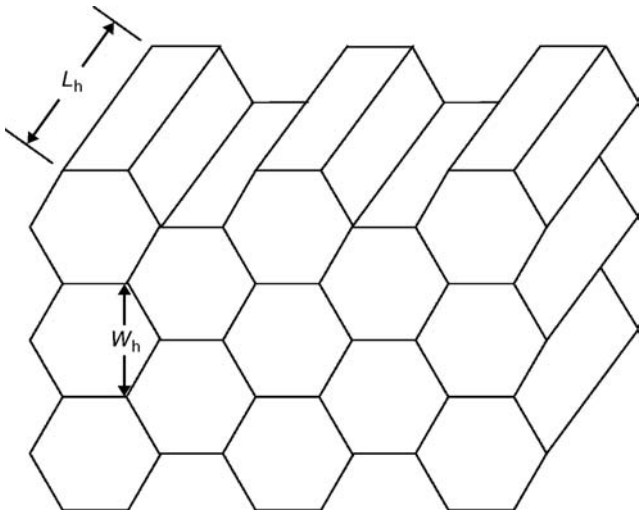

Figure 3. Schematic of a hexagonal honeycomb section.

Honeycomb removes swirl from the incoming flow and minimizes the lateral variations in both mean and fluctuating velocity (Mehta and Bradshaw, 1979). The yaw angle for the incoming flow should be less than 10° to avoid stalling of the honeycomb cells. Honeycomb comes in different shapes such as circular, square, and hexagonal cross sections. Among these, hexagonal is usually the cross-sectional shape of choice, as it has the lowest pressure drop coefficient (Barlow, Rae and Pope, 1999). Honeycomb cells have been shown to have the best performance with a length-to-diameter ratio of between 7 and 10 (Mehta and Bradshaw, 1979). Mehta and Bradshaw (1979) also state that the cell size should be smaller than the smallest lateral wavelength of the velocity variation. The honeycomb section should have sufficient structural rigidity to withstand applied forces during operation without significant deformation. Special consideration may be required if the incoming Mach number to the honeycomb section is high enough that flow choking is possible.

Tensioned screens are placed in the settling duct for the reduction of turbulence levels of the incoming flow. Screens break up the large-scale turbulent eddies into a number of small-scale eddies that subsequently decay. Schubauer, Spangenberg and Klebanoff (1950) state that the Reynolds number based on the screen wire diameter should be less than 60 to prevent additional turbulence generation due to vortex shedding.

The spacing between the screens should be of the order of the length scale of the large energy-containing eddies (Mehta and Bradshaw, 1979). Placing multiple screens in the settling duct with varying porosity, with the coarsest screen being closest to the incoming flow and the finest screen being closest to the test section, has been shown to provide lower values of test section turbulence (Watmuff, 1998). A settling chamber is necessary after the screens so the smaller-scale fluctuations generated by the wires can decay before accelerating through the contraction.

3.2.2 Contraction

The inlet contraction plays a critical role in determining the flow quality in the test section. The contraction accelerates and aligns the flow into the test section. The size and shape of the contraction dictate the final turbulence intensity levels in the test section (Derbunivich *et al*., 1987). The contraction stretches vortex filaments, which reduces axial but intensifies lateral turbulent fluctuations (Tennekes and Lumley, 1972). The length of the contraction should be sufficiently small to minimize boundary-layer growth and cost but long enough to prevent large adverse pressure gradients along the wall, generated by streamline curvature, which can

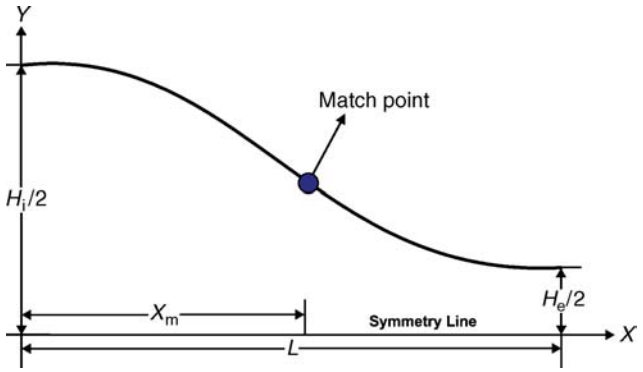

Figure 4. Schematic of the contraction shape with matched polynomials.

lead to flow separation. While CFD may be used in modern design schemes, Morel (1975) suggested a simple analytical method of matched polynomials. A schematic of the contraction shape polynomial is shown in Figure 4. The entrance height of the contraction is H_i, and the exit height is H_e. The total length of the contraction is L, and the two polynomials are matched (location, slope, and curvature) at a specified location $x = x_m$. At the exit of the contraction, any remaining "free" higher-order derivatives of the polynomial are set to zero to obtain a straight section.

In particular, Su (1992) recommended matching a cubic polynomial at the contraction entrance with a higher-order polynomial at the contraction exit. Contractions with minimal flow nonuniformities can be designed by iteratively selecting the entrance height, contraction ratio, match point, and length of the contraction. Techniques using 3-D potential flow simulations inside the contraction followed by the application Stratford's (1958) separation criteria for turbulent boundary layers affected by adverse pressure gradients can be applied to develop optimized contractions meeting design criteria for test section flow uniformity (Mathew, 2005).

3.2.3 *Test section*

The test section can be of the closed-wall or the open-jet type. The test section design should allow for ease of accessibility and installation of wind-tunnel test models and instrumentation. Aerodynamic performance of the models can be better matched to full-scale performance in a closed test section; however, an open jet permits far-field acoustic measurements at the cost of potential test section jet deflection, jet/collector interactions, and shear layer refraction (Amiet, 1978). In a closed-wall test section, acoustic measurements suffer from poor signal-to-noise ratios due to [usually] turbulent boundary-layer pressure fluctuations and acoustic reverberation. The facility's primary design purpose should determine which test section type is used. For 2-D studies, the chord should not exceed $\frac{1}{3} \sim \frac{2}{3}$ span (Barlow, Rae and Pope, 1999). It is also essential to have a blockage ratio of $<10\%$ based on the frontal area of the model (Barlow, Rae and Pope, 1999). A common rule of thumb in test section sizing is to have rectangular dimensions with a ratio of about 1.4–1 (Bradshaw and Mehta, 2003).

3.2.4 *Diffuser*

The diffuser decelerates the high-speed flow from the test section, thereby achieving static pressure recovery and reducing the load of the drive system. The flow field within the diffuser is influenced by the nature of the flow leaving the test section. The orientation, size (blockage), and wake development of the airfoil models are some of the factors that affect the diffuser entrance flow. The area of the diffuser should increase gradually along its axis, so as to prevent flow separation. As with contraction sections, diffuser geometry can be optimized.

Barlow, Rae and Pope (1999) state that for a conical diffuser, the divergence half angle of the diffuser walls should be less than 3.5° for a "good" design. Mehta (1977) states that the diffuser-included angle for a conical diffuser should be between 5° (for best flow steadiness) and 10° (for best pressure recovery). Klines' flat diffuser curves (Runstadler, Dolan and Dean, 1975) are generally used for the (non-CFD-based) design of diffusers, as shown in Figure 5. The area ratio AR between the exit and entrance of the diffuser is plotted versus the ratio of diffuser length to the entrance height of the diffuser. Three regions are shown on the plot. The design of the

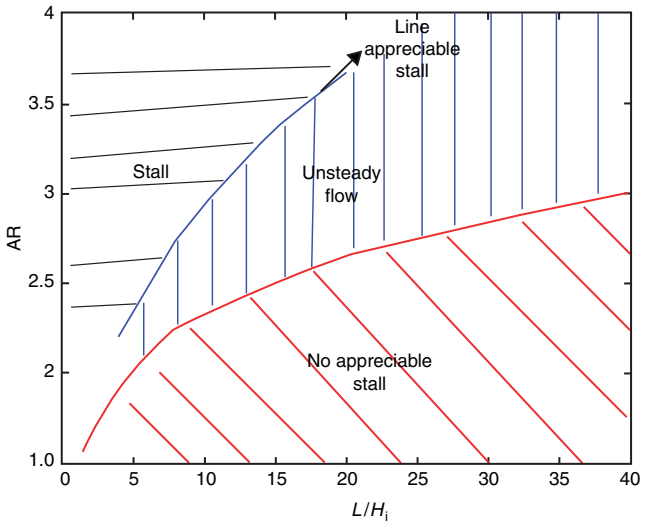

Figure 5. 2-D diffuser design curves. Adapted from Runstadler, Dolan and Dean (1975) © Creare, Inc.

diffuser is conducted by selecting a length for the diffuser, that is, within facility size constraints. Given L/H_i (where the height is dictated by the test section size), the corresponding value of AR is selected from the no-stall regions. Although a greater pressure recovery can be achieved by operating in the "unsteady flow" regime, this can contribute to unwanted noise, as well as poor performance at off-design flow conditions. If facility constraints limit the length of the diffuser or a closed-circuit design is used, a turning section with guide vanes can be used, and the diffuser can be broken into multiple sections.

3.2.5 *Drive system selection*

The drive system generates a volume flow rate and compensates for the remaining pressure losses. The driver can be a fan, blower, or a regulated compressed gas source. The relative advantages and disadvantages are discussed in Section 2.1.

Fans are rated by the volume flow rate and the static pressure drop they can overcome. Barlow, Rae and Pope (1999) provide a procedure for estimation of the losses incurred in the tunnel circuit, aiding in fan selection.

Fan performance is characterized by fan load curves that are plots of fan efficiency and pressure loss as a function of flow rate (Figure 6). Load curves are estimated for various fan rotational speeds. The pressure loss calculation (Barlow, Rae and Pope, 1999) leads to the wind-tunnel performance curve, which is an estimate of the static pressure loss for various values of volume flow rates. The points where the pressure loss curves intersect the tunnel performance curve determine the operating points of the wind tunnel. Fans provide optimal performance when the tunnel operating points fall near the maximum efficiency of the fan, as shown in Figure 6.

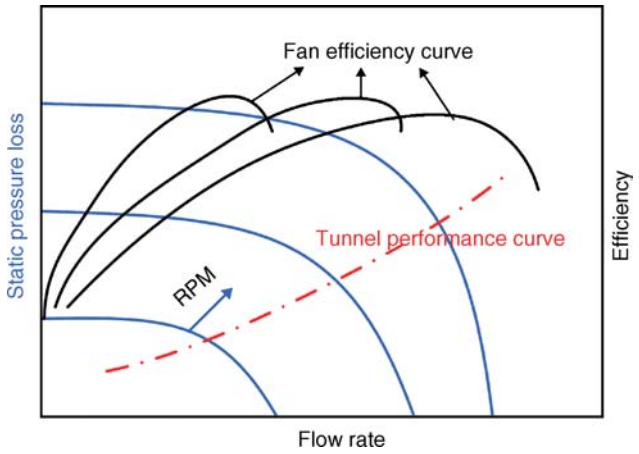

Figure 6. Fan load curve.

One of the main components of background noise comes from the fan or drive system. When designing a low-disturbance facility, fan noise must be attenuated. The blade passage frequency (BPF $= R \cdot N_{\text{blades}}$) and its harmonics appear as discrete tones in the test section background noise spectra at a fixed tunnel speed and may contaminate sensor measurements and affect flow physics. A spectrogram (contour plots of sensor signal power vs. frequency) obtained via short-time discrete Fourier transforms as the tunnel speed is increased is an effective tool to reveal blade passage contamination (Duell *et al.*, 2004). Such contamination can be reduced via acoustic treatment of the tunnel circuit and other acoustic paths (in open-circuit case) between the fan and test section.

3.2.6 *Optional components*

For an open-jet test section, a collector is required at the downstream end of the test section to capture the jet. The resulting flow pattern is highly dependent on the room characteristics and the test configuration/conditions. The area of the collector is a design parameter that is best determined via CFD. The negative aspects of the collector include noise due to boundary-layer "scrubbing" and turbulent shear layer impingement on the collector. The collector is acoustically treated in an acoustic wind tunnel. Its effect on flow and acoustic measurements requires careful assessment.

In closed-circuit tunnels where the ducts are joined together by 90° bends, flow separation will occur, leading to significant pressure drop, flow unsteadiness, and noise generation. Turning vanes are installed in corner sections to mitigate these adverse effects. Collar (1937) and Salter (1946) developed some early designs for turning vanes. Gelder *et al.* (1986) developed turning vanes with a low loss factor. The chord, thickness-to-chord ratio, shape, and the number of turning vanes determine the efficiency, as defined by flow losses, of the turning section. Modern CFD can now be used to design advanced turning vanes that function well over the entire speed range of the tunnel. In addition, the turning vanes offer the possibility for cooling (or heating) the flow via heat transfer between the tunnel flow and fluid passing through the vane interior.

Mechanical vibrations generated by the drive system can propagate into the test section through ductwork and the ground. These vibrations must be minimized if aero-optic, transition, or acoustic measurements will be conducted. Vibration isolation devices consist of passive and active mounts, as well as a flexible bellows section (Beranek and Vér, 1992; Mathew, 2005).

4 FACILITY CHARACTERIZATION

A wind tunnel must be characterized to determine if the design criteria are satisfied. The most obvious test is to check that the facility operates safely at desired flow speeds, but beyond this a series of careful experiments are recommended. Some of the most common characterization experiments are in the text below.

4.1 Flow uniformity

Clearly, uniform velocity in the test section is desired. The inviscid core of the test section flow should have as little deviation from a plug profile as possible. There are a large number of experimental techniques available to measure the mean velocity profile (Tavoularis, 2005), including traversing a pitot-static or pitot probe through the test section (see Pressure and Velocity Measurements). This is a proven, inexpensive, but time-consuming technique. A rake may be used as an alternative, so multiple spatial locations can be measured simultaneously. Single or multiple hot wires configured for constant-temperature anemometry (CTA), particle image velocimetry (PIV), and laser Doppler velocimetry (LDV) can also be used. The flow uniformity is usually characterized as either as a min–max or an rms deviation from the mean velocity in the inviscid core flow of the test section (Mathew, 2005).

4.2 Turbulence characterization

For many facilities, low turbulence levels in the test section are critical. While many full-scale applications may have significant incoming turbulence levels, wind-tunnel tests often seek to isolate the effects of incoming freestream turbulence. For example, in boundary-layer transition studies, significant levels of incoming turbulence can alter the behavior of the boundary-layer transition location. In aeroacoustic studies, ingested turbulence can interact with model components and generate additional "leading edge" noise, contaminating measurements of other components of interest, such as airfoil trailing edge noise (Brooks, Pope and Marcolini, 1989).

As an unsteady velocity measurement, test section turbulence levels are well suited for evaluation using constant-temperature hot wire anemometry (Bruun, 1995). A single hot wire can be traversed through the core of the test section, and the bridge signal measured and analyzed at each spatial location. Note that a single hot wire will resolve a velocity magnitude normal to the wire line, with ambiguous angle of incidence, while rejecting velocity fluctuations along the axis of the wire. It should also be noted that in most wind tunnels, test section turbulence is anisotropic (Bradshaw and Mehta, 2003), meaning the axial and lateral fluctuations can be drastically different. As such, a measurement scheme should be used to resolve these two different velocity components. In the simplest configuration, a measurement can be conducted with a single wire normal to the incoming flow, and then the wire can be rotated such that the test section axial fluctuations would be rejected in a repeated experiment. However, if two simultaneous velocity components are desired, a dual-wire probe configuration is usually used. For complete velocity steady and unsteady vector decomposition, a triple wire assembly is required. These configurations are shown in Figure 7. An array of hot wires can be used if spatial–temporal data or wave number spectra are desired. Turbulence intensity (TI) is typically computed as in equation (1) (expressed as a percent of the local mean velocity). When computing TI, it is common to high-pass filter the data at some cut-on frequency related to the mean flow speed and test section size to separate true turbulence from large-scale facility unsteadiness, such as $f > V_\infty/(2L_{\mathrm{TS}})$ (Bradshaw and Mehta, 2003). Velocity spectra can be evaluated. An alternative method uses LDV, although it requires flow seeding that must faithfully follow the turbulent flow (Tavoularis, 2005). LDV can be used in single-, dual- (as shown in Figure 8), or triple-beam configurations to resolve one, two, or three components of velocity. PIV provides 2-D or 3-D (if stereo) data in a plane, enabling the computation of time-averaged statistics. For more information on CTA, LDV, and PIV, see Thermal Anemometry: An Introduction and Special Topics, Laser Doppler Velocimetry, and Particle Image Velocimetry.

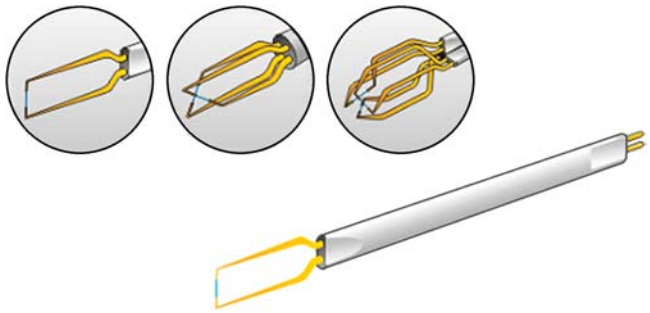

Figure 7. Single-, dual-, and triple-wire CTA configurations. Reproduced with permission from Dantec Dynamics (2009).

$$\mathrm{TI} = \frac{u'}{V} \tag{1}$$

4.3 Acoustics and vibration

If the facility is used for acoustic measurements, background noise should be assessed. Ideally, an aeroacoustic flow facility should have background noise levels at least 10 dB below the acoustic source of interest in a test (Duell *et al.*, 2002),

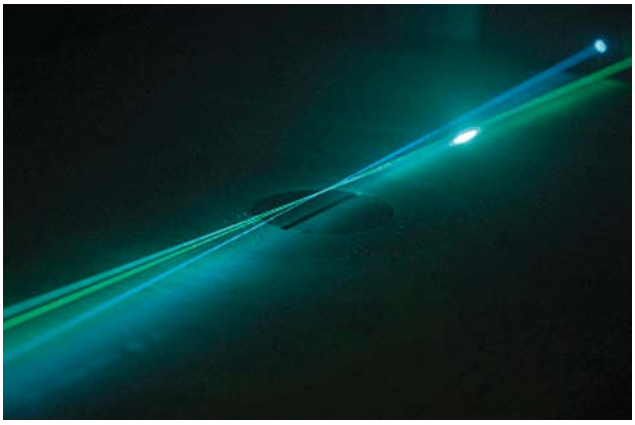

Figure 8. Two-beam LDV configuration for two-component velocity measurements. Reproduced with permission from R. Holman (2006) © University of Florida.

but this is rarely the case. Many measurement techniques are available for analyzing acoustic sources contaminated by background noise (Soderman and Allen, 2002), but all benefit from minimizing background noise levels as much as possible.

Background noise levels are commonly measured using a single free-field microphone. This microphone can either be placed in the inviscid core of the test section (using a nose cone), flush mounted in the wall of a closed-wall test section, or outside of the flow in an open-jet test section facility. The selection is typically based on where the majority of acoustic measurements will be made. If the overall sound pressure level (OASPL) is the quantity of interest, appropriate frequency bounds should be selected for the power integration. For common applications where frequency shifts to full scale are not a concern, A-weighting is often used (Duell *et al*., 2002).

Vibration measurements can be conducted using single- or multi-axis accelerometers (Beranek and Vér, 1992). Absolute vibration levels can be evaluated. If any steps have been taken in the facility design and fabrication to mitigate vibration transmission through duct treatments, a transmission loss factor can be measured. This relates the vibration from a source, such as the tunnel drive system, to the vibration in the facility test section through correlation and coherence analysis.

5 CONCLUSIONS

Wind tunnels are an essential tool used by experimentalists to complement analytical and computational methods. A wide variety of wind-tunnel facilities exist, since tunnel design is highly dependent on the application of interest. Tunnel design is an iterative process that must address various competing constraints and requirements. Completed facilities must be carefully characterized to determine their characteristics.

RELATED CHAPTERS

The Role of Wind Tunnel Experiments in CFD Validation
Flow Visualization by Direct Injection Technique
Optical Flow Visualization
Shear Stress Measurements
Spectroscopic and Scattering Techniques
Temperature and Heat Transfer Measurements
Measurement of Aerodynamic Forces and Moments in Wind Tunnels

NOMENCLATURE

A	cross-sectional area (m^2)
a	isentropic speed of sound ($m\,s^{-1}$)
BPF	blade passage frequency (Hz)
c_p	constant pressure specific heat ($J\,kg^{-1}\,K^{-1}$)
Ec	Eckert number $V^2/c_p\Delta T$
Eu	Euler number $(p - p_\infty)/\rho V^2$
f	frequency (Hz)
Fr	Froude number V^2/gL
g	gravitational acceleration ($m\,s^{-2}$)
H_e	duct exit height (m)
H_i	duct inlet height (m)
k	thermal conductivity ($W\,m^{-1}\,K^{-1}$)
L	reference length scale (m)
M	Mach number V/a_∞
N_{blades}	number of fan blades
p	pressure (Pa)
Pr	Prandtl number $\mu c_p/k$
R	fan rotation rate (Hz)
Re	Reynolds number $\rho VL/\mu$
St	Strouhal number fL/V
V	reference velocity magnitude ($m\,s^{-1}$)
x	streamwise location in contraction (m)
ΔT	temperature difference (K)
TI	turbulence intensity
U	local mean velocity magnitude ($m\,s^{-1}$)
u'	local root mean square fluctuating velocity magnitude ($m\,s^{-1}$)
μ	dynamic viscosity ($kg\,m^{-1}\,s^{-1}$)
ρ	density ($kg\,m^{-3}$)

SUBSCRIPTS

TS	test section property
∞	freestream conditions

REFERENCES

Amiet, R.K. (1978) Refraction of sound by a shear layer. *J. Sound Vib.*, **58**(4), 467–482.

Barlow, J.B., Rae, W.H. Jr. and Pope, A. (1999) *Low-Speed Wind Tunnel Testing*, 3rd edn, John Wiley and Sons, New York.

Beranek, L.L. and Vér, I.L. (1992) *Noise and Vibration Control Engineering – Principles and Applications*, John Wiley & Sons, New York.

Brooks, T.F., Pope, D.S. and Marcolini, M.A. (1989) Airfoil self noise and prediction. NASA Reference Publication 1218, July 1989.

Bruun, H.H. (1995) *Hot-Wire Anemometry, Principles and Signal Analysis*, Oxford University Press, New York.

Bradshaw, P. and Mehta, R. (2003) Wind Tunnel Design, http://www-htgl.stanford.edu/bradshaw/tunnel/ (accessed 18 June 2009).

Choi, K. and Simpson, R.L. (1987) Some mean velocity, turbulence and unsteadiness characteristics of the VPI & SU stability wind tunnel. *Report VPI-Aero-161*, December 1987.

Collar, A.R. (1937) Some experiments with cascades of aerofoils. A.R.C., Reports and Memoranda. *Technical Report 1768*.

Dantec Dynamics (2009) http://www.dantecdynamics.com/Default.aspx?ID=1057.

Derbunivich, G.I., Zemskaya, A.S., Repik, E.U. and Sosedko, Y.P. (1987) Effect of flow contraction on the level of turbulence. *Izv. Akad. Nauk SSSR Mekh. Zhidk. Gaza*, **2**, 146–152.

Duell, E., Walter, J., Arnette, S. and Yen, J. (2002) Recent advances in large-scale aeroacoustic wind tunnels. 8th AIAA/CEAS Aeroacoustics Conference and Exhibit. AIAA Paper 2002-2503. Breckenridge, Colorado, June 2002.

Duell, E., Yen, J., Walter, J. and Arenette, S. (2004) Boundary layer noise in aeroacoustic wind tunnels. 42nd AIAA Aerospace Sciences Conference. AIAA Paper 2004-1028. Reno, Nevada, January 2004.

Gelder, T.F., Moore, R.D., Sanz, J.M. and McFarland, E.R. (1986) Wind tunnel turning vanes of modern design. 24th Aerospace Science Meeting. AIAA Paper 86-0044. Reno, Nevada, January 1986.

Holman, R., (2006). An experimental investigation of flows from zero-net mass-flux actuators. PhD. MAE Department, University of Florida.

Mathew, J. (2005) Design, fabrication and characterization of an anechoic wind tunnel facility. PhD. MAE Department, University of Florida.

Mehta, R.D. (1977) The aerodynamic design of blower tunnels with wide angle diffusers. *Progr. Aerosp. Sci.*, **18**, 59–120.

Mehta, R.D. and Bradshaw, P. (1979) Design rules for small low speed wind tunnels. *Aeronaut. J.*, **83**, 443–449.

Morel T. (1975) Comprehensive design of axisymmetric wind tunnel contractions. *J. Fluids Eng.*, **97**(2), 225–233.

Mueller, T.J., Scharpf, D.F., Batill, S.M., Sullivan, C.J. and Subramanian, S. (1992) The design of a subsonic low-noise low turbulence wind tunnel for acoustic measurements. AIAA 17th Aerospace Ground Testing Conference. AIAA Paper 92-3883. Nashville, Tennessee, July 1992.

NASA Aeronautics Test Program (2007a) NASA's Aeronautics Test Program 11-Foot Transonic Unitary Plan Facility, http://www.aeronautics.nasa.gov/atp/facilities/documents/06ames11x11_dsi.pdf (accessed 18 June 2009).

NASA Aeronautics Test Program (2007b) NASA's Aeronautics Test Program 14×22 Foot Subsonic Tunnel, http://www.aeronautics.nasa.gov/atp/facilities/documents/03langley14x22_dsi.pdf (Accessed 18 June 2009).

NASA Aeronautics Test Program (2007c) National Transonic Facility, http://www.aeronautics.nasa.gov/atp/facilities/documents/07langleyntf_dsi.pdf (accessed 18 June 2009).

NASA Langley Research Center (2006) The Langley 20-Inch Supersonic Wind Tunnel, http://wte.larc.nasa.gov/facilities_updated/fluid_dynamics/20inch_supersonic2.htm (accessed 18 June 2009).

Naval Warfare Center Carderock Division (2009) Towing Basins, http://www.dt.navy.mil/hyd/fac/tow-bas/index.html (accessed 21 July 2009).

The Pennsylvania State University (2007) Garfield Thomas Water Tunnel Facilities, http://www.arl.psu.edu/facilities/gtwt.html (accessed 18 June 2009).

Pope, A. and Goin, K.L. (1965) *High-Speed Wind Tunnel Testing*, John Wiley & Sons, New York.

Rasmi, S. (2002) Characterization of the University of Florida air–water shear layer facility. M.S., MAE Department, University of Florida.

Runstadler, P.W., Dolan, F.X. and Dean, R.C. (1975) *Diffuser Data Book*, Creare, Inc. Hanover, New Hampshire.

Salter, C. (1946) Experiments on thin turning vanes. A.R.C., Reports and Memoranda, no. 2469.

Schubauer, G.B., Spangenberg, W.G. and Klebanoff, P.S. (1950) Aerodynamic characteristics of damping screens. *NACA TN 2001*.

Saric, W.S., Reed, H.L. and White, E.B. (2003) Stability and transition of three-dimensional boundary layers. *Annu. Rev. Fluid Mech.*, **35**, 413–440.

Soderman, P.T. and Allen, C.S. (2002) Microphone measurements in and out of airstream (Chapter 1), in *Aeroacoustic Measurements* (ed. T.J. Mueller), Springer-Verlag, Berlin, Heidelberg & New York.

Stratford, B.S. (1958) The prediction of separation of the turbulent boundary layer. *J. Fluid Mech.*, **5**, 1–16.

Su, Y. (1992) Flow analysis & design of three-dimensional wind tunnel contractions. *AIAA J.*, **29**(11), 1912–1919.

Tavoularis, S. (2005) *Measurements in Fluid Mechanics*, Cambridge University Press, New York.

Tennekes, H. and Lumley, J.L. (1972) *A First Course in Turbulence*, MIT Press, Cambridge, Massachusetts.

Watmuff, J.H. (1998) Detrimental effects of almost immeasurably small freestream nonuniformities generated by wind-tunnel screen. *AIAA J.*, **36**(3), 379–386.